Journal of The Electrochemical Society

Structural and Electrochemical Investigation of Fe_xSi_{1-x} Thin Films in Li Cells

Structural and Electrochemical Investigation of Fe_xSi_{1-x} Thin Films in Li Cells

Zhijia Du,[a] R. A. Dunlap,[a,b,c] and M. N. Obrovac[a,b,d,*,z]

[a]*Department of Physics and Atmospheric Science, Dalhousie University, Halifax, Nova Scotia B3H 4R2, Canada*
[b]*Institute for Research in Materials, Dalhousie University, Halifax, Nova Scotia B3H 4R2, Canada*
[c]*College of Sustainability, Dalhousie University, Halifax, Nova Scotia B3H 4R2, Canada*
[d]*Department of Chemistry, Dalhousie University, Halifax, Nova Scotia B3H 4R2, Canada*

Fe_xSi_{1-x} thin films with $0 \leq x \leq 0.46$ have been prepared by combinatorial sputtering and their electrochemical properties have been studied in Li half-cells. X-ray diffraction showed that all of the films had an amorphous structure. Mössbauer effect spectra suggest that Fe was diluted in amorphous Si for $x \leq 0.23$ and inactive $FeSi_2$ was formed with further increase in x. For $x \leq 0.23$, all Si in the thin films was active toward lithiation/delithiation. At higher Fe contents, the capacity of Fe-Si thin films dropped rapidly and no capacity was observed for x greater than 0.33. The voltage curve of Si to become depressed during lithiation with increasing Fe content, which may be the result of stress induced between the active Si phase and inactive phases in the alloy. For alloys with $x > 0.23$, the formation of inactive $FeSi_2$ removes active Si from the alloy and results in the lowering of the reversible capacity.
 [DOI: 10.1149/2.0961609jes]

Manuscript submitted April 28, 2016; revised manuscript received June 17, 2016. Published July 20, 2016.

Si alloys have received a great deal of research effort as the negative electrode materials for Li-ion batteries. The use of Si alloys, instead of pure Si, dilutes the volume expansion to acceptable degree, and therefore increases cycling performance.[1,2] Models have shown that a-Si/inactive alloy could result in ~22% energy density improvement of cell stack with about 100% volume expansion (compared to 34% improvement with 280% volume expansion).[2] Thus, binary TM-Si alloys (where TM is a transition metal element that is inactive with lithium) such as Cr-Si, Fe-Si, Ni-Si, Mn-Si and Co-Si,[3–7] have been widely studied as negative electrode materials in the last two decades.

Fe-Si is one of the most studied TM-Si systems. Fleischauer et al. investigated TM-Si alloy systems (TM = Fe, Mn, Cr+Ni) using high-throughput combinatorial sputtering.[4] They observed that the capacity of TM-Si alloys decreased with increasing TM content, and suggested that these films comprise an active Si phase and an inactive transition metal silicide phase. A modified effective heat of formation (EHF) model was used by Fleischauer et al. to explain the capacity-composition trend in Fe-Si in terms of the co-existence of amorphous Si and inactive FeSi.[5] McGraw et al. studied the microstructure of Fe-Si thin films by X-ray diffraction and ^{57}Fe Mössbauer spectroscopy.[8] Fe was diluted in amorphous Si for Fe less than 12 at% as observed by a decrease in Mössbauer center shift with increasing Fe content. For Fe content from 12 at% to 47 at%, the thin film was assumed to consist of a two-phase region of diluted Fe in amorphous Si and nanocrystalline FeSi because the observed center shift and quadrupole splitting approached the values of crystalline FeSi. However, the similar hyperfine parameters for FeSi and $FeSi_2$ made the distinction between these phases difficult, and the conclusion that FeSi formed instead of $FeSi_2$ was ultimately based on the electrochemical properties previously reported by Fleischauer et al.[4]

Recently we have reported that the voltage curve of Si in active/inactive Si alloys can be significantly affected by the inactive phase and suggested that stress-voltage coupling was responsible.[6] In such alloys the active Si phase expands during lithiation, while the inactive phase does not. This can cause large internal stresses which can depress the voltage of the active Si phase significantly during lithiation.[6,9] Indeed, voltage shifts from stress-voltage coupling are clearly visible in the results of Fleischauer et al.,[4] but they are not discussed. Unfortunately, Fleischauer et al. used cyclic voltammetry in their electrochemical characterization of alloy systems, which resulted in each cell being cycled at variable rates. Therefore, a meaningful analysis of the voltage shifts apparent in Reference 4 is not possible. In contrast to the EHF model proposed by Fleischauer et al., by taking stress-voltage coupling into account and using galvanostatic cycling, we recently found that for sputtered Ni-Si thin films, all Si atoms are active for all alloy compositions in this alloy system. Therefore, no silicide phase is formed at all in this system. Instead, the observed decrease in capacity with increasing Ni content originates from the voltage depression of the Si phase due to stress-voltage coupling between inactive Ni and active Si during lithiation.[6]

Considering that previous results did not take into account that the inactive phase can significantly shift the voltage of Si raises important questions. Namely, if the models proposed in previous studies accurately reflect the effect of the inactive phase on alloy capacity. Another question to be answered is whether different inactive phases shift the voltage of Si by different amounts, which would be an important consideration in cell design. Therefore, it is important to systematically re-investigate the binary Fe-Si system in order to quantify voltage shifts from stress-voltage coupling and to take this into account when modeling alloy capacity. In the present study, combinatorial sputtering was used, as previously,[4,8] to produce Fe-Si thin films with a large range of compositions. The electrochemistry of these films was studied in Li cells and their microstructures were investigated by X-ray diffraction and Mössbauer effect spectroscopy.

Experimental

Thin film libraries of Fe-Si were fabricated using a modified Corona Vacuum System V3-T sputtering system as described previously.[10] The chamber pressure was maintained at about 1.2 mTorr argon during the deposition. 50 mm diameter targets of Si (99.9% purity, Pure Tech,) and Fe (99.5% purity, Aesar) were used. Two Fe_xSi_{1-x} libraries denoted as Library I ($0 \leq x \leq 0.42$) and Library II ($0.17 \leq x \leq 0.46$) were prepared using a constant mask for the Si target, a linear-out mask for one Fe target, and a constant mask for a second Fe target (for Library II). The detailed sputtering parameters were listed in Table I.

Fe_xSi_{1-x} films were deposited on Cu foil disks (Furukawa Electric Co., Japan) with an area of 1.27 cm^2, a Si (111) wafer, a copper-coated glass plate and 15 Kapton substrates (32 × 105 mm in size). The loading mass of Fe_xSi_{1-x} alloy was measured by weighing the Cu disks with a Sartorious SE-2 microbalance (0.1 μg precision) before and after sputter deposition. X-ray diffraction (XRD) patterns of films deposited on Si (111) wafers were collected using a JD2000

*Electrochemical Society Member.
[z]E-mail: mnobrovac@dal.ca

Table I. Summary of the sputtering parameters presented in this work.

	Deposition Power (W) / Deposition Time (hr) / Covering mask		
Library	Si	Fe	Fe
Library I	140 / 9 / Constant	40 / 9 / Linear in	N/A
Library II	150 / 8 / Constant	30 / 8 / Linear in	13 / 8 / Constant

diffractometer equipped with a Cu-K_α X-ray source and a diffracted beam monochromator. Composition data were collected using a JEOL 8200 microprobe from measurements of samples sputtered on Cu coated glass plates. Room temperature ^{57}Fe Mössbauer effect spectra were collected using a Wissel System II spectrometer operating in the constant acceleration mode and a ^{57}Co source. The velocity scales were referenced to room temperature α-Fe. Data were accumulated by means of an Ortec multichannel scaler using ACE-MCS software. A portion of the film corresponding to a small composition range was positioned between the source and detector (over which a slit aperture was placed).

Cu foil disks with sputtered thin films were assembled into 2325 coin cells with Li metal (99.9%, Sigma-Aldrich) counter electrodes and 1 M $LiPF_6$ (BASF) in EC/DEC/FEC (3:6:1 v/v/v, Novolyte Technologies) electrolyte in an Ar-filled glove box. The electrodes were separated by two layers of Celgard 2301 separator. Cells were cycled at 30 ± 0.1°C with a Maccor Series 4000 Automated Test System. A rate of C/10 rate was used for the 1st cycle and a C/5 rate for the following cycles, with a C/20 trickle discharge during the lithiation half-cycle. C-rate was calculated from trial cells as reported previously.[6]

Results and Discussion

Figure 1 shows the composition library closure for Fe_xSi_{1-x} Library I. The top panel shows the theoretical amount of sputtered Fe and Si from the linear mask and constant mask, respectively. The middle panel shows the atomic fraction of Fe and Si from electron microprobe measurements, which agrees well with lines calculated from the top panel. The bottom panel shows that the measured mass of the sputtered films fits well with the calculated mass from top panel. This shows that the compositions measured by electron microprobe and by mass are completely consistent with each other. A similar analysis was used to determine the composition range obtained in Library II.

The XRD patterns of $Fe_{0.10}Si_{0.90}$, $Fe_{0.25}Si_{0.75}$ and $Fe_{0.40}Si_{0.60}$ thin films are shown in Figure 2. All the patterns have two broad diffraction peaks at around 28° and 49°, indicating the amorphous/nanocrystalline structure of sputtered Fe-Si thin films. With increasing Fe content, the intensity of the peak at 49° increases and its position shifts slightly to lower angle. All Fe-Si thin films in this study were amorphous/nanocrystalline, which is similar to previous reports.[4,6]

Mössbauer effect spectra were measured for sputtered Fe-Si thin films to further investigate their microstructure and selected spectra are illustrated in Figure 3. All spectra contain a quadrupole split doublet. Each spectrum was fit into a Voigt-based function corresponding to a single Gaussian distribution of quadrupole split doublets as was used by McGraw et al., who also studied sputtered Si-Fe thin films by Mössbauer effect spectroscopy.[8] Figure 4 and Figure 5 display the mean room temperature center shift and mean quadrupole splitting of the quadrupole split spectra, respectively. For $x < 0.23$, the Fe_xSi_{1-x} thin films show a decrease in center shift with increasing Fe content. The increasing Fe content increases the average number of Fe near neighbors for a Fe probe nucleus. This leads to the decreasing center shift due to an increase in the s-electron density at the Fe nuclei. Since the XRD patterns show no crystalline features, this region may be considered as "dilute Fe in amorphous Si", as previously reported for alloys with Fe content less than 12 at% by McGraw et al.[8] Here this Fe-Si solid solution region extends significantly further to Fe contents as high as 23 at%. According to the equilibrium Fe-Si phase diagram,

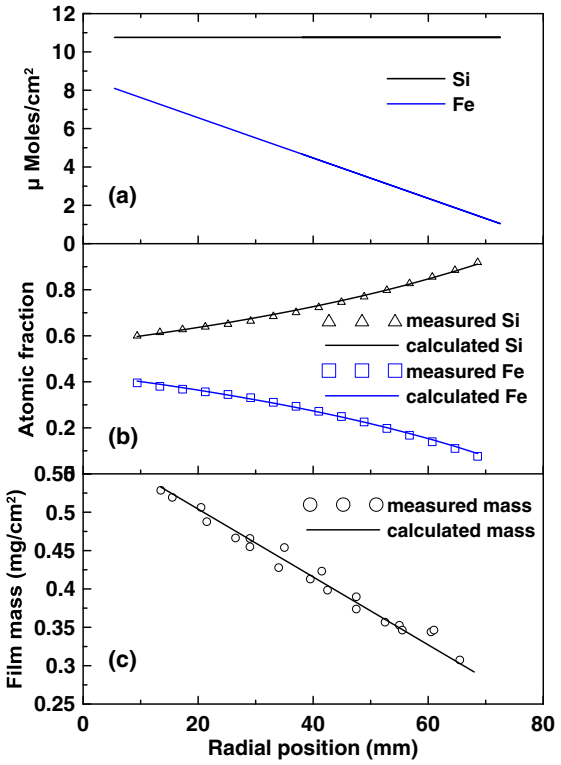

Figure 1. Library closure of the Fe_xSi_{1-x} thin films in Library I. (a) theoretical number of moles of Fe and Si sputtered per unit area as defined by the sputtering masks, (b) atomic fraction of Si and Fe in the Fe_xSi_{1-x} thin films as measured by electron microprobe and its theoretical value based on panel (a), (c) the measured mass of the sputtered film and the calculated mass per unit area (based on panel (a)).

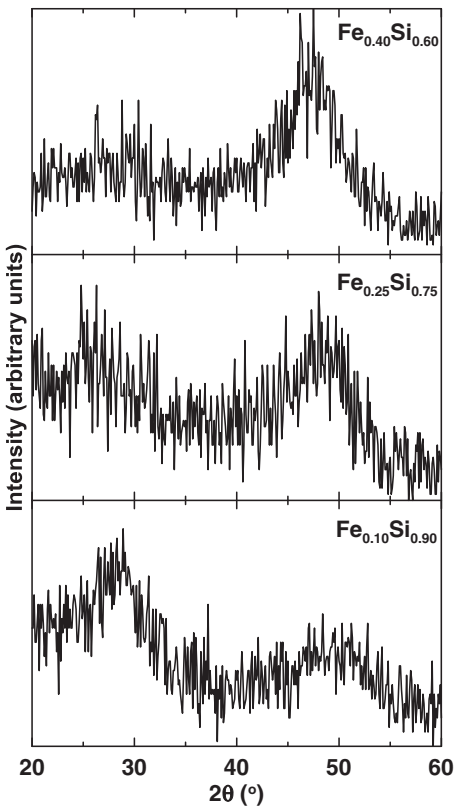

Figure 2. XRD patterns of $Fe_{0.10}Si_{0.90}$, $Fe_{0.25}Si_{0.75}$, $Fe_{0.40}Si_{0.60}$ thin films deposited on Si (100) wafers.

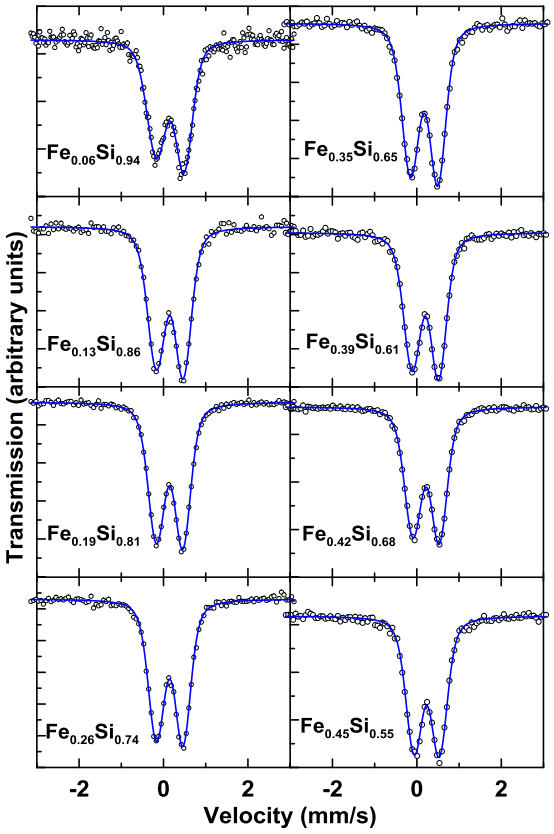

Figure 3. Room temperature ^{57}Fe Mössbauer effect spectra of Fe_xSi_{1-x} thin films. Fits to distributions of quadrupole doublets as described in the text are illustrated by the solid lines.

Fe has almost no solid solubility in Si. Therefore, the observed Fe-Si solid solution region in sputtered films is a metastable state. As such, its extent is likely to be highly variable, depending on the sputtering conditions.

For alloys with x > 0.23, the center shift becomes progressively more positive. This can be the result of the co-existence of a two phase region consisting of dilute Fe in amorphous Si and nanocrystalline Fe-Si compounds ($FeSi_2$ and/or FeSi) where the fraction of the latter phase increases with increasing Fe content. However, the exact distinction between $FeSi_2$ and FeSi is difficult on the basis of Mössbauer measurements alone because $FeSi_2$ has a very similar center shift to FeSi.[8,11–13] The mean quadrupole splitting in Figure 5 shows relatively little variation as a function of composition. The phenomenon is very similar to the result reported by McGraw et al. because the mean local electric field gradient is dominated by the structural ordering of the amorphous phase.[8] This is verified by the XRD patterns that show that all sputtered thin films in this composition range are amorphous. The identification of the silicide phase that is formed will be discussed below, in the context of electrochemical measurements.

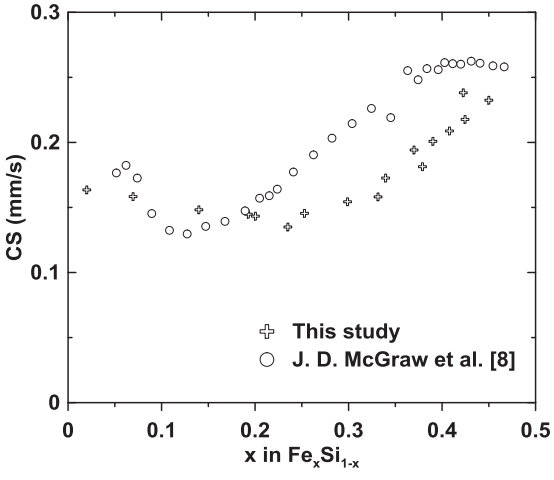

Figure 4. Mean center shift relative to room temperature α-Fe (CS) for all spectra that were fit to a distribution of doublets as a function of x in Fe_xSi_{1-x} thin films. Also shown are data from the study by McGraw et al.[8]

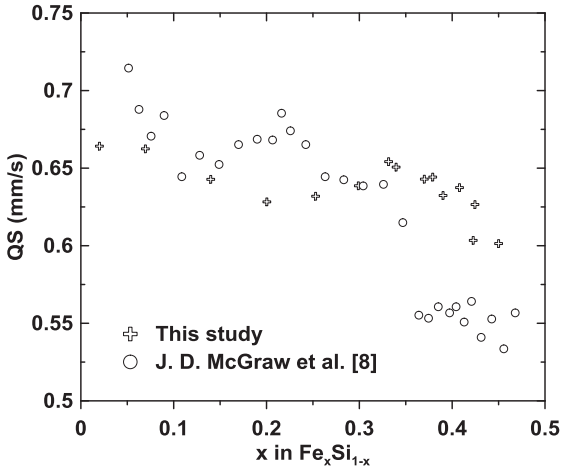

Figure 5. Mean quadrupole splitting (QS) for all spectra that were fit to a distribution of doublets as a function of x in Fe_xSi_{1-x} thin films. Also shown are data from the study by McGraw et al.[8]

Figure 6 shows the voltage curves of sputtered Fe-Si thin films for the first three cycles. All the voltage curves are characteristic of amorphous Si alloys with sloping plateaus during the lithiation and delithiation processes. The lithiation voltage of the first cycle

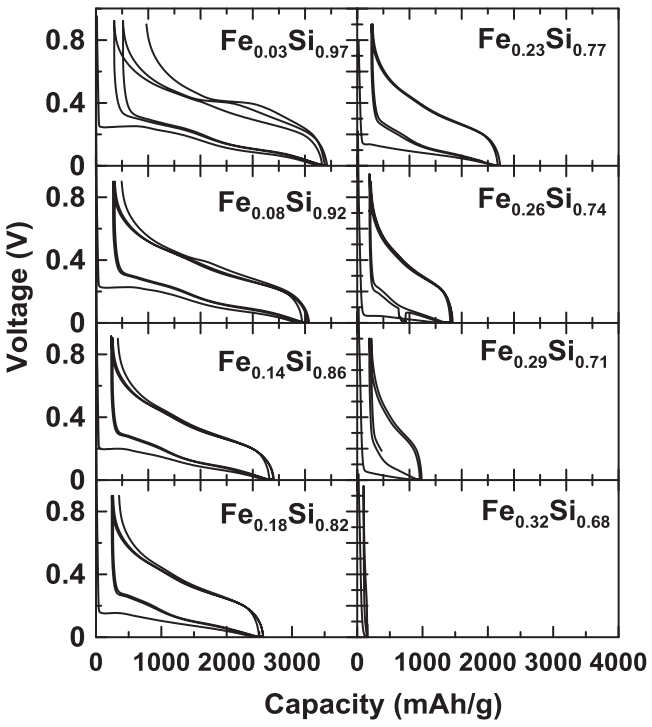

Figure 6. Voltage versus capacity curves of thin films with selected compositions.

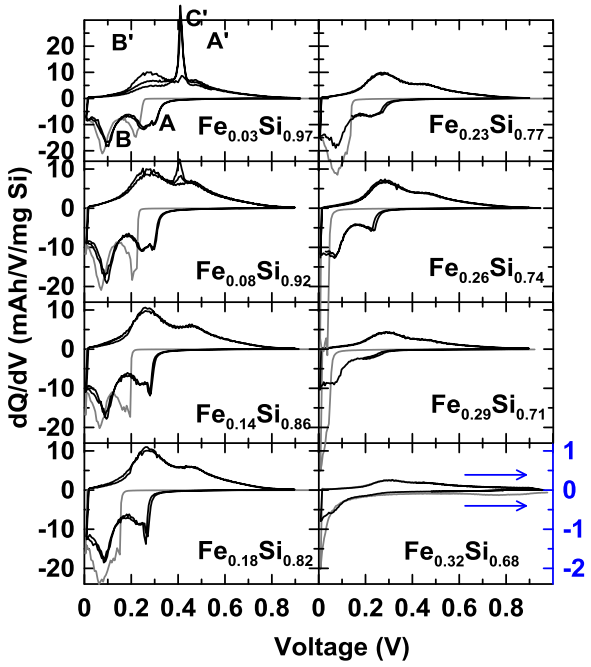

Figure 7. Differential capacity curves for cells shown in Figure 2.

is gradually depressed with increasing Fe content. The $Fe_{0.03}Si_{0.97}$ thin film shows a flat plateau at about 0.42 V during the 2nd and 3rd delithiation half-cycles, which is related to the crystalline $Li_{15}Si_4$ phase. The $Li_{15}S_4$ phase related plateau occurs for the 3rd cycle for $Fe_{0.08}Si_{0.92}$ thin film. For thin films with higher Fe content, there is no 0.42 V plateau during delithiation for the first three cycles. This results from the absence of $Li_{15}Si_4$ phase formation due to the depression of the lithiation voltage by an inactive phase in Si alloys as reported in our recent publications.[6,7] No appreciable reversible capacity can be observed for thin films with Fe content higher than 33 at%. This is in contrast to the previous report by Fleischauer et al.,[4] in which the Fe-Si thin films were active for compositions up to 40 at% Fe. We believe this can be attributed to differences in the sputtering conditions, which may affect the composition ranges of metastable phases, as mentioned above.

Figure 7 shows the differential capacity curves (per mg Si) of the first three cycles derived from Figure 6. The first lithiation process is shown in gray in order to distinguish it from subsequent cycles. During the first lithiation, lithiation does not proceed until a low threshold voltage is reached. We attribute this to a nucleation and growth process, which is common during the first lithiation of alloys.[2] During the second lithiation cycle, a sharp peak occurs at about 0.28 V for some compositions and may also correspond to a nucleation and growth process for the lithiation of the fully delithiated alloy. This peak is followed by two broad peaks, here labeled A and B, corresponding to the two single phase lithiation processes that occur for amorphous Si. The positions of peak A and peak B shift to lower voltages as the Fe content in the alloy is increased. We ascribe the voltage depression during lithiation to the stress-voltage coupling phenomena as reported for Si thin films[9] and for the Ni-Si system.[6] In the Ni-Si system, it was shown that when a trickle discharge is used, stress-voltage coupling can cause the capacity to decrease when peaks in the differential capacity become shifted below the lower voltage cutoff. This does not occur here for any composition. Therefore, the capacity measured here should relate to compositional changes and should not be effected by shifts in voltage due to internal particle stress.

During delithiation, two peaks (labeled A′ and B′ in Figure 7) are present in the differential capacity and correspond to the two single-phase delithiation processes that occur during the delithiation of amorphous Si. A sharp peak, (labeled C′ in Figure 7) for the $Fe_{0.03}Si_{0.97}$ and $Fe_{0.08}Si_{0.92}$ compositions forms after the second cycle and continually grows with cycling. This peak is related to the formation of the $Li_{15}Si_4$ phase. As Fe content is increased, causing increased compressive stress on the active Si phase during lithiation, peaks A and B shift to lower voltages, causing the complete suppression of the $Li_{15}Si_4$ phase. This same effect occurs in the Ni-Si system.[6] Therefore, the presence of the $Li_{15}Si_4$ peak for small x is an indicator that the active Si phase is not bonded to an inactive phase. Unlike peaks A and B which shift due to compressive stresses during lithiation, peaks B′ and A′ do not change position with increasing Fe content. This may be due to the release of tensile stress by fracturing. The same phenomenon has been suggested to occur in the Ni-Si system.[6]

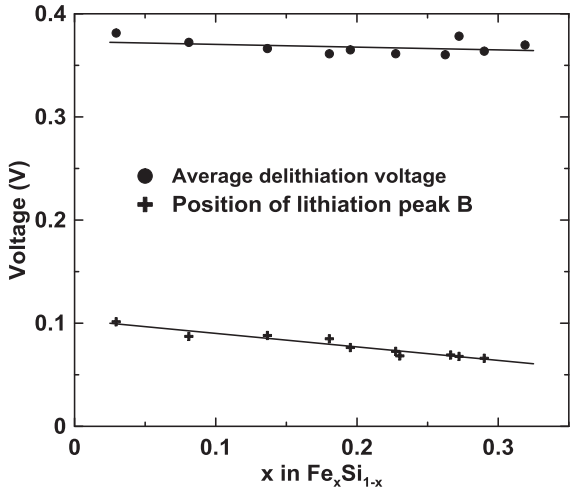

Figure 8. Average second cycle delithiation voltage and position of the lithiation peak B versus the Fe_xSi_{1-x} thin film composition.

Figure 8 shows the average delithiation voltage of the 2nd cycle for Fe-Si thin film electrodes. In contrast to delithiation, the average lithiation voltage is not a good representation of the voltage behavior of the A and B peaks during lithiation. This is because a peak from a nucleation/growth process is present in the differential capacity curves at about 0.3 V during lithiation. This process would tend to lower the average lithiation voltage, even if peaks A and B remained unchanged. Therefore, instead of plotting the average lithiation voltage, the position of the peak B is shown instead. In addition, the differential capacity curves of the 2nd cycle are superimposed on each other in Figure 9 to clarify the shift in voltage with Fe content. As is apparent

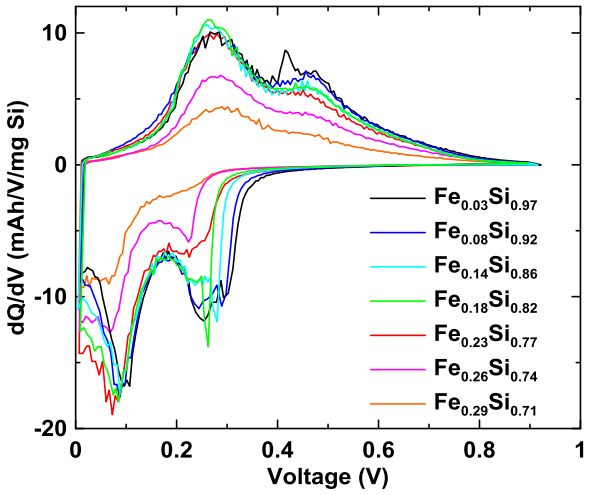

Figure 9. Superposition of the second cycle differential capacity curves of Fe_xSi_{1-x} thin films.

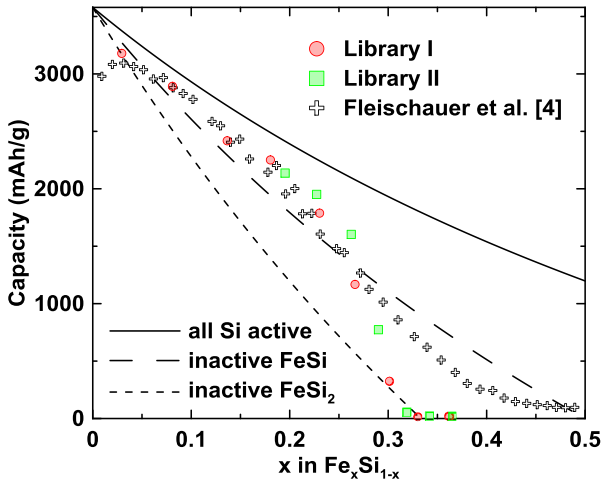

Figure 10. The first reversible capacity of Fe_xSi_{1-x} thin films as measured for Fe-Si thin film Libraries I and II. Also shown are data from the study by Fleischauer et al.[4] The curves in the figure representing the theoretical capacity if all the Si is active (solid line) and if Fe reacts with Si to form inactive $FeSi_2$ (dashed line).

in Figures 8 and 9, the position of peak B shifts to lower voltage with increasing Fe content. This feature can be attributed to the voltage depression by inactive Fe, similar to the voltage-stress coupling phenomena in Ni-Si system.[6] The average delithiation voltage is nearly unchanged versus Fe content. This behavior similar to what we observed for the Ni-Si system.[6] We speculate that this is due to stress release in the film due to plastic deformation and/or film fracture. Also notable from Figure 8 is that there are no discontinuities in the average voltage as a function of composition, which would be indicative of differential capacity peaks being truncated at the low voltage cutoff during lithiation.[6] This is further evidence that the capacity measured here is not affected by stress-voltage coupling for any composition.

Figure 10 shows the initial reversible capacity of the Fe-Si thin films versus x in Fe_xSi_{1-x}. Also shown are the results of Fleischauer et al. from Reference 6. For $x \leq 0.23$, the capacity agrees very well with that measured by Fleischauer et al. Also shown in Figure 7 are lines corresponding to the theoretical capacities of the Fe_xSi_{1-x} alloys if all the Si is active, if inactive $FeSi_2$ is formed or if inactive FeSi is formed, the latter model being the one suggested by Fleischauer et al.[4] According to the Mössbauer analysis above, our thin films should comprise Si and Fe phases for Fe contents less than 23 at%. Therefore, all the Si should be active for these compositions. Instead, the capacity is slightly lower than the model in which all the Si is active and slightly higher than the model in which FeSi is formed as an inactive phase. It is reasonable that the capacity should be lower than its theoretical value because of the huge volume changes that occur during cycling, resulting in capacity loss due to mechanical degradation. For the same reason it is not likely that the capacity should be higher than its theoretical value. Therefore, the capacity is consistent with all the Si being active for Fe contents less than 23 at% based on Mössbauer and electrochemical results.

With further increase in x above 0.23, the capacity of the thin film decreases rapidly until no capacity is observed for the sample with $x = 0.33$. Since the capacity decrease is not ascribed to stress-induced voltage depression, as discussed above, it suggests that $FeSi_2$, which is inactive toward lithium, is formed in the thin film. Also taking into account Mössbauer and XRD results, it is concluded that Fe_xSi_{1-x} thin films with $0.23 \leq x \leq 0.33$ comprise Fe, amorphous Si, and nanocrystalline $FeSi_2$. The presence of $FeSi_2$ has also been demonstrated by anomalous small-angle X-ray scattering studies of sputtered Fe-Si thin films.[14] At $x = 0.33$ the film is comprised only of nanocrystalline $FeSi_2$, which is electrochemically inactive. For $0.33 \leq x \leq 0.46$, the thin film may consist of nanocrystalline $FeSi_2$ and nanocrystalline FeSi, which is also expected to be inactive toward lithiation/delithiation.

For compositions above $x = 0.23$ the capacity reported for Fe-Si thin films by Fleischauer et al. also begins to decrease rapidly, as shown in Figure 10. However, the capacity of Fleischauer et al. does not decrease as rapidly as for our films. One reason for this discrepancy could arise from variations in the sputtering conditions and in the combinatorial cell used by Fleischauer et al., in which it was found that the Cu leads contribute to the observed reversible capacity.[4] Indeed, in the data from Fleischauer et al. the Fe-Si thin films actually never become inactive, but instead have capacities above 50 mAh/g, even at high Fe contents. In addition, there is a definite change in behavior for films at about $x = 0.23$, with films with $x < 0.23$ being consistent with all Si being active and films with $x > 0.25$ being consistent with an inactive Fe-Si phase forming. Therefore, a simple explanation of the capacity based solely on the formation of a Si/FeSi active/inactive alloy as proposed by Fleischauer et al. does not seem reasonable. Instead, the above results suggest that the inactive phase is Fe metal when $x < 0.23$, and Fe and $FeSi_2$ are the active phases present when $0.23 \leq x < 0.33$. Further research is needed to verify the behavior of other Si-transition metal alloy systems, so that voltage shifts due to stress-voltage coupling and careful determination of capacity trends can be quantified.

Conclusions

Amorphous Fe_xSi_{1-x} ($0 \leq x \leq 0.46$) thin films were prepared by combinatorial sputtering and the effect of Fe content on microstructure and electrochemistry was investigated. XRD patterns of the films suggest that they have an amorphous/nanocrystalline microstructure. Mössbauer effect spectra suggest that a Fe phase is diluted in amorphous Si for $x \leq 0.23$ and that inactive $FeSi_2$ begins to form with further increases in Fe content. All of the voltage curves in Li cells show sloping plateaus for the first cycle during lithiation/delithiation, which is characteristic of amorphous Si alloys. Increasing Fe content results in the depression of the lithiation voltage curve, consistent with stress-voltage coupling. Features in the voltage curve related to $Li_{15}Si_4$ formation occur for $x \leq 0.10$ after three cycles. For higher Fe contents, no $Li_{15}Si_4$ related features are observed due to the lithiation voltage depression by inactive Fe. The capacity-composition analysis suggest that all Si is active for $x \leq 0.23$ and some Si becomes deactivated for higher Fe contents. No active Si is observed for x greater than 0.33. These results suggest that the inactive phase is Fe metal when $x < 0.23$, a mixture of Fe and $FeSi_2$ when $x > 0.23$, and $FeSi_2$ when $x = 0.33$.

Acknowledgments

The authors acknowledge funding from NSERC and 3 M Canada, Co. under the auspices of the Industrial Research Chair program. We also acknowledge the support of the Canada Foundation for Innovation, the Atlantic Innovation Fund and other partners that fund the Facilities for Materials Characterization managed by the Institute for Research in Materials. ZD acknowledges financial support from the Killam Trusts.

References

1. M. N. Obrovac, L. Christensen, D. B. Le, and J. R. Dahn, *J. Electrochem. Soc.*, **154**, A849 (2007).
2. M. N. Obrovac and V. L. Chevrier, *Chem. Rev.*, **114** (23), 11444 (2014).
3. A. Netz, R. A. Huggins, and W. Weppner, *J. Power Sources*, **119-121**, 95 (2003).
4. M. D. Fleischauer, J. M. Topple, and J. R. Dahn, *Electrochem. Solid-State Lett*, **8**(2), A137 (2005).
5. M D. Fleischauer, R. Mar, and J. R. Dahn, *J. Electrochem. Soc.*, **154**(3), A151 (2007).
6. Z. Du, T. D. Hatchard, R. A. Dunlap, and M. N. Obrovac, *J. Electrochem. Soc.*, **162**(9), A1858 (2015).
7. Z. Du, S. N. Ellis, R. A. Dunlap, and M. N. Obrovac, *J. Electrochem. Soc.*, **163**, A13 (2016).
8. J. D. McGraw, M. D. Fleischauer, J. R. Dahn, and R. A. Dunlap, *Philos. Mag.*, **86**(32), 5017 (2006).

9. D. S. M. Iaboni and M. N. Obrovac, *J. Electrochem. Soc.*, **163**(2), A255 (2016).
10. J. R. Dahn, S. Trussler, T. D. Hatchard, A. Bonakdarpour, J. N. Meuller-Neuhaus, K. C. Hewitt, and M. Fleischauer, *Chem. Mater.*, **14**, 3519 (2002).
11. K. Vojtěchovský and T. Zemčík, *Czech. J. Phys. B*, **24**, 171 (1974).
12. Ö. Helgason and T. I. Sigfússon, *Hyperfine Interact.*, **45**, 415 (1989).
13. J. Desimoni and F. H. Sánchez, *Hyperfine Interact.*, **122**, 277 (1999).
14. M. B. Fernández van Raap, M. J. Regan, and A. Bienenstock, *J. Non-Cryst. Solids*, **191**, 155 (1995).